

## Structure of a $^{129}\text{Xe}$ -Cryptophane Biosensor Complexed with Human Carbonic Anhydrase II

Julie A. Aaron, Jennifer M. Chambers, Kevin M. Jude, Luigi Di Costanzo, Ivan J. Dmochowski, and David W. Christianson\*

Roy and Diana Vagelos Laboratories, Department of Chemistry, University of Pennsylvania, Philadelphia, Pennsylvania 19104-6323

Received March 27, 2008; E-mail: chris@sas.upenn.edu

The  $\alpha$ -carbonic anhydrases (CAs) are zinc metalloenzymes that catalyze the reversible hydration of  $\text{CO}_2$  in forming  $\text{HCO}_3^-$ . The active site of an  $\alpha$ -CA contains a catalytically essential  $\text{Zn}^{2+}$  coordinated by three histidine residues at the bottom of a 15 Å deep cleft, and the tightest binding CA inhibitors developed to date contain a sulfonamide moiety that coordinates to  $\text{Zn}^{2+}$  as a sulfonamidate anion.<sup>1</sup> Notably, human isozyme II (CAII) is an ideal model system for exploring new inhibitor designs, some of which can be exploited in biosensing applications.<sup>2–4</sup> Here, CAII is utilized for the structure-based design of a xenon ( $^{129}\text{Xe}$ ) biosensor for potential use as a magnetic resonance imaging (MRI) contrast agent.

The  $^{129}\text{Xe}$  isotope has a spin-1/2 nucleus, a >200 ppm chemical shift window in water, and a natural isotopic abundance of 26% (commercially available up to 86%), which makes it an appealing biomolecular probe for MRI. Moreover,  $^{129}\text{Xe}$  can be laser polarized to enhance MRI signals  $\sim 10\,000$ -fold.<sup>5</sup> Although current in vivo MRI applications are limited to functional lung imaging through the diffusion of Xe gas,<sup>6</sup> the encapsulation of  $^{129}\text{Xe}$  within a cryptophane cage ( $K_D \approx 30\ \mu\text{M}$  at 37 °C in phosphate-buffered solution)<sup>7</sup> facilitates its use as a biosensor that can be targeted to specific proteins using an appropriate affinity tag.<sup>8,9</sup> For example, racemic biosensor **1** (Figure 1a) has been designed to bind to the CA isozymes ( $K_D = 60 \pm 20\ \text{nM}$  against CAII in solution) and yields a distinctive  $^{129}\text{Xe}$ -MRI spectrum when bound to CAII.<sup>10</sup> Here, we report the X-ray crystal structure of the CAII-**1**-Xe complex at 1.70 Å resolution.

For structure determination, CAII was overexpressed in *Escherichia coli* and purified as described,<sup>11</sup> then incubated with a 2-fold excess of **1**, concentrated to 10 mg/mL, and crystallized by the hanging drop vapor diffusion method. Crystals were cryoprotected in 15% glycerol and subsequently pressurized under 20 atm Xe for 30 min prior to flash cooling and X-ray data collection. The structure was refined to final  $R_{\text{work}}$  and  $R_{\text{free}}$  values of 0.23 and 0.25, respectively.

Biosensor **1** coordinates to the active site  $\text{Zn}^{2+}$  ion as the sulfonamidate anion, displacing the zinc-bound hydroxide ion of the native enzyme as previously observed in other complexes of CAII with benzenesulfonamide derivatives.<sup>1,2,12</sup> The crystallographic occupancies of **1** and  $\text{Zn}^{2+}$  are refined at 0.5. It is unusual to observe diminished  $\text{Zn}^{2+}$  occupancy in a CAII inhibitor complex, but the molecular origins of this effect are not clear.

The encapsulation of Xe within the cryptophane cage of **1** is confirmed by inspection of the Bijvoet difference Fourier map calculated from anomalous scattering data (Figures 1b and S1 in Supporting Information). X-ray diffraction data were collected at a wavelength  $\lambda = 0.9795\ \text{\AA}$ , which is far from the Xe  $L_1$  edge of 2.27 Å.<sup>13</sup> Nevertheless, the anomalous scattering component  $f''$  is 3.4  $e^-$  for Xe, so the anomalous signal is still prominent at the wavelength of data collection. A second Xe binding site is observed

in a hydrophobic pocket defined by A116, L148, V218, L157, V223, and F226 (Figure S2). The crystallographic occupancies of these Xe sites refine to 0.50 and 0.37, respectively. Anomalous scattering peaks are absent from crystals not subject to Xe pressurization.

Notably, **1** contains a chiral axis, and the electron density map reveals the binding of equal populations of both enantiomers (each refined with an occupancy of 0.25; Figure 1).<sup>14–16</sup> Overall, the binding of **1** does not cause any significant structural changes in the active site, and the root-mean-square deviation is 0.34 Å for 256 C $\alpha$  atoms between the current structure and the unliganded enzyme (PDB 2CBA).<sup>17</sup>

The total surface area of **1** is  $\sim 1500\ \text{\AA}^2$ , of which  $\sim 500\ \text{\AA}^2$  becomes solvent inaccessible due to contacts of **1** within the active site cleft of CAII designated molecule I in Figure 2. The surrounding CAII molecules in the unit cell (molecules II–IV) sequester an additional  $\sim 540\ \text{\AA}^2$  of the surface area of **1** from solvent. Some structural changes are observed near the outer rim of the active site cleft where the cryptophane binds. The most notable change is observed for Q136, which rotates  $\sim 180^\circ$  to make van der Waals contacts with the cryptophane and the symmetry-related cryptophane bound to molecule III in the crystal lattice. Other residues at the active site rim of molecule I that make close contacts with the cryptophane are G132 and P202. Additional structural changes in the crystal lattice result from the binding of **1** to molecule I: in molecule II, H36 rotates  $\sim 90^\circ$  to make a van der Waals contact with the cage, and Q137 of molecule III rotates  $\sim 90^\circ$  to donate a hydrogen bond to an ether oxygen atom of **1**.

Although the pendant propionates appear to be more disordered than the cryptophane and are characterized by correspondingly weaker electron density, a hydrogen bond between a propionate moiety and Q53 of molecule II is observed. The relative dearth of strong cryptophane–protein interactions may explain why the affinity of **1** measured by ITC is only slightly better than that measured for the parent triazole benzenesulfonamide lacking the cryptophane ( $K_D = 100 \pm 10\ \text{nM}$ ).<sup>10</sup>

Limited hydrogen bond interactions between CAII and the cryptophane moiety of **1** may be advantageous for the use of cryptophanes as  $^{129}\text{Xe}$  biosensors. Translational and rotational freedom, the consequence of a flexible linker between the cryptophane and the benzenesulfonamide, could allow the cage to reorient rapidly in situ, independently of the protein, to result in decreased correlation times and narrower line widths that increase the sensitivity of  $^{129}\text{Xe}$  NMR measurements in solution.<sup>8</sup>

In conclusion, this work reveals the first experimentally determined structure showing how an encapsulated  $^{129}\text{Xe}$  atom can be specifically directed to a biomedically relevant protein target. The possible implications for cancer diagnosis are profound, given that CA isozymes IX and XII are overexpressed on the surface of certain cancer cells.<sup>18</sup> Moreover, a search of the Protein Data Bank reveals

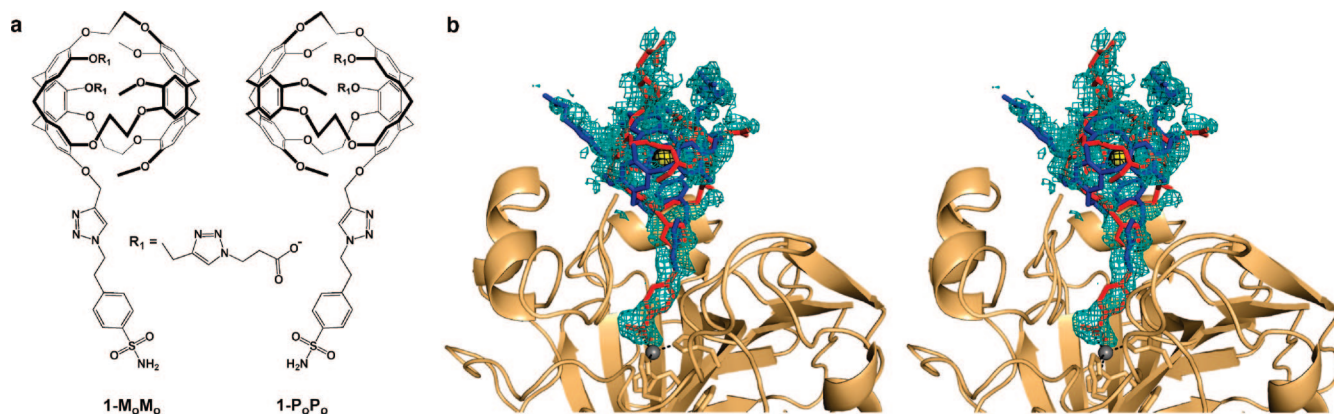


**Figure 1.** (a) The  $M_0M_0$  and  $P_0P_0$  enantiomers of the cryptophane-A-derived CA biosensor. The benzenesulfonamide moiety serves as an affinity tag that targets the  $Zn^{2+}$  ion, and the  $R_1$  substituents contain triazole propionate moieties that enhance aqueous solubility. (b) Stereoview of a simulated annealing omit map showing  $1-M_0M_0$  (blue) and  $1-P_0P_0$  (red) bound in the active site ( $1.9 \sigma$  contour, teal). A Bijvoet difference Fourier map ( $2.0 \sigma$ , black) confirms the encapsulation of Xe (yellow). Coordination interactions with  $Zn^{2+}$  (gray sphere) are indicated by dotted lines.

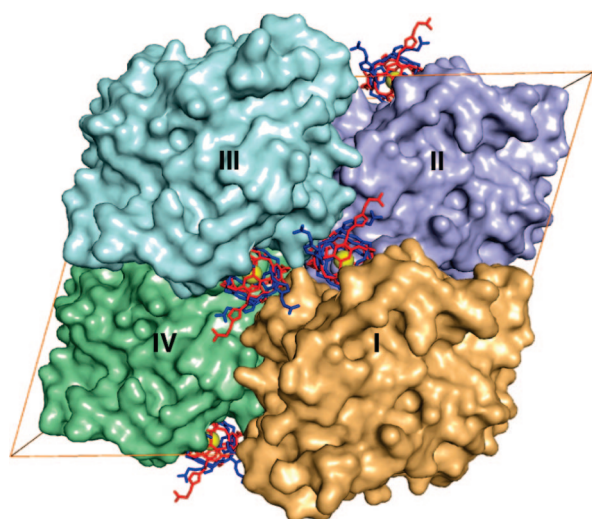


**Figure 2.** The unit cell of CAII crystals in space group  $C2$  contains four molecules: I ( $x, y, z$ ), II ( $x + 1/2, y + 1/2, z$ ), III ( $-x, y, -z$ ), and IV ( $-x + 1/2, y + 1/2, -z$ ). The binding of **1** in the active site cleft of molecule I buries  $\sim 500 \text{ \AA}^2$ . Crystal contacts bury an additional  $540 \text{ \AA}^2$  of the surface of **1** as follows:  $270 \text{ \AA}^2$  with molecule III, and  $240$  and  $30 \text{ \AA}^2$  with the front and back faces of molecule II, respectively. Molecule IV does not contact **1** bound to molecule I.

that, with its molecular mass of 1554, the **1**-Xe complex is one of the largest synthetic organic ligands ever cocrystallized with a protein. Thus, this work demonstrates the feasibility of preparing crystalline complexes between proteins and nonbiological, nanometer-scale ligands.<sup>19</sup>

**Acknowledgment.** We thank the Advanced Light Source and the Cornell High Energy Synchrotron Source beamline F-2 for access to X-ray crystallographic data collection facilities, and Ulrich English for support with the Xe chamber experiments. We also thank P.A. Hill for helpful discussions. I.J.D. is a Camille and Henry Dreyfus Teacher-Scholar and thanks DOD for Grant W81XWH-04-1-0657. Finally, we thank the NIH for a Chemical Biology

Interface training grant (to J.A.A.), 1R21CA110104 (to I.J.D.), and GM49758 (to D.W.C.). D.W.C. also thanks the BBSRC for the Underwood Fellowship.

**Supporting Information Available:** Experimental procedures and crystallographic data. This material is available free of charge via the Internet at <http://pubs.acs.org>.

## References

- Supuran, C. T.; Scozzafava, A. *Bioorg. Med. Chem.* **2007**, *15*, 4336–4350.
- Elbaum, D.; Nair, S. K.; Patchan, M. W.; Thompson, R. B.; Christianson, D. W. *J. Am. Chem. Soc.* **1996**, *118*, 8381–8387.
- Krishnamurthy, V. M.; Kaufman, G. K.; Urbach, A. R.; Gitlin, I.; Gudiksen, K. L.; Weibel, D. B.; Whitesides, G. M. *Chem. Rev.* **2008**, *108*, 946–1051.
- Bozym, R. A.; Thompson, R. B.; Stoddard, A. K.; Fierke, C. A. *ACS Chem. Biol.* **2006**, *1*, 103–111.
- Cherubini, A.; Bifone, A. *Prog. Nucl. Magn. Reson. Spectrosc.* **2003**, *42*, 1–30.
- Fain, S. B.; Korosec, F. R.; Holmes, J. H.; O'Halloran, R.; Sorkness, R. L.; Grist, T. M. *J. Magn. Reson. Imaging* **2007**, *25*, 910–923.
- Hill, P. A.; Wei, Q.; Eckenhoff, R. G.; Dmochowski, I. J. *J. Am. Chem. Soc.* **2007**, *129*, 9262–9263.
- Lowery, T. J.; Garcia, S.; Chavez, L.; Ruiz, E. J.; Wu, T.; Brotin, T.; Dutasta, J. P.; King, D. S.; Schultz, P. G.; Pines, A.; Wemmer, D. E. *ChemBioChem* **2006**, *7*, 65–73.
- Schröder, L.; Lowery, T. J.; Hilty, C.; Wemmer, D. E.; Pines, A. *Science* **2006**, *314*, 446–449.
- Chambers, J. M.; Hill, P. A.; Aaron, J. A.; Han, Z.; Christianson, D. W.; Kuzma, N. N.; Dmochowski, I. J. Manuscript in preparation.
- Alexander, R. S.; Kiefer, L. L.; Fierke, C. A.; Christianson, D. W. *Biochemistry* **1993**, *32*, 1510–1518.
- Eriksson, A. E.; Kylsten, P. M.; Jones, T. A.; Liljas, A. *Proteins: Struct. Funct. Genet.* **1988**, *4*, 283–293.
- Watanabe, T. *Phys. Rev.* **1965**, *137*, 1380–1382.
- Collet, A. In *Comprehensive Supramolecular Chemistry*; Atwood, J. L., Davis, J. E. D., MacNicol, D. D., Vogtle, F., Eds.; Pergamon: New York, 1996; Vol. 2, Chapter 11, pp 325–365.
- Ruiz, E. J.; Sears, D. N.; Pines, A.; Jameson, C. J. *J. Am. Chem. Soc.* **2006**, *128*, 16980–16988.
- Eliel, E. L.; Wilen, S. H. *Stereochemistry of Organic Compounds*; John Wiley & Sons, Inc.: New York, 1994; pp 1119–1190.
- Håkansson, K.; Carlsson, M.; Svensson, L. A.; Liljas, A. *J. Mol. Biol.* **1992**, *227*, 1192–1204.
- Pastorekova, S.; Parkkila, S.; Zavada, J. *Adv. Clin. Chem.* **2006**, *42*, 167–216.
- The atomic coordinates of the human carbonic anhydrase II–sulfonamide cryptophane-A complex have been deposited in the Protein Data Bank with accession code 3CYU.

JA802214X